EVALUATION OF RATE-BASED FORCE-REFLECTING TELEOPERATION IN FREE MOTION AND CONTACT

Robert L. Williams II
Jason M. Henry
Department of Mechanical Engineering
Ohio University
Athens, OH 45701

Daniel W. Repperger
AFRL / HECP
Wright-Patterson AFB, OH 45433

PRESENCE: Teleoperators and Virtual Environments
Vol. 9, No. 1, pp. 25-36, February 2000

Contact author information:
Robert L. Williams II
Assistant Professor
Department of Mechanical Engineering
257 Stocker Center
Ohio University
Athens, OH 45701-2979
phone: (740) 593-1096
fax: (750) 593-0476
e-mail: bobw@bobcat.ent.ohiou.edu
URL: http://www.ent.ohiou.edu/~bobw

EVALUATION OF RATE-BASED FORCE-REFLECTING TELEOPERATION IN FREE MOTION AND CONTACT

Robert L. Williams II[1], **Jason M. Henry**[2]
Mechanical Engineering
Ohio University
Athens, OH 45701

Daniel W. Repperger[3]
AFRL / HECP
Wright-Patterson AFB, OH 45433

ABSTRACT

This research focuses on improved force-reflecting teleoperation system control in free motion and contact tasks. Specifically, the Naturally-Transitioning Rate-to-Force Controller (*NTRFC*) is implemented in an Air Force experimental force-reflecting teleoperation system to: 1) achieve a unified controller with no mode switches from free motion to contact; and 2) reduce the wrench exerted on the environment by the slave manipulator during remote teleoperation tasks. In an effectiveness evaluation experiment, the experimental hypothesis is validated: the *NTRFC* with force reflection performs the best amongst four teleoperation control modes with respect to minimal wrench exertion on the environment. A negligible difference was found in total task completion times amongst the four modes. The *NTRFC* with force reflection has the potential to improve task performance in remote hazardous teleoperation tasks where minimal exerted wrench is desirable.

[1] Assistant Professor
[2] Graduate Research Assistant
[3] Civilian Researcher

INTRODUCTION

There are many tasks that require human reasoning and improvisation to complete, but the task environment may be hazardous or inaccessible by humans. Teleoperation of a remote manipulator allows a person to perform these tasks safely. Rate control can be an effective method of teleoperation because it allows for very large movements of the slave with small movements of the master. The resolved-rate algorithm is also attractive because it is a linearized, unique solution (assuming full rank for the Jacobian matrix), and control inputs from various sources can be summed linearly to form the total input command. One main reason why rate control has not been widely used for teleoperation is the problem of contacting the environment. If a rate is commanded while the slave is in contact with the environment the slave will try to push through the environment, and the contact forces increase to unacceptably large values. This can result in damage to the slave or the environment. The free-motion-to-contact problem under rate control is the primary focus of this article.

Many solutions have been proposed to solve the problem of contacting the environment via a remote manipulator. Raibert and Craig (1981) presented a hybrid control method wherein some Cartesian axes are controlled in position while the remaining axes are force controlled. While this method can be effective in practical tasks, one must choose either position or force on each Cartesian axis. Hogan (1985) presented an impedance controller where the behavior of a manipulator is controlled to mimic a 6-degree-of-freedom (dof) Cartesian *m*-*c*-*k* system, but it requires a switch to go from free motion to constrained motion. Colbaugh et al. (1993) present an adaptive scheme for controlling the end-effector impedance of robot manipulators in contact; however, an explicit control mode change is required for free motion. Hyde and Cutkosky (1994) experimentally evaluate several methods for controlling the transition from free motion to constrained motion, using a one-axis impact testbed. Yao and Tomizuka (1995) present an adaptive motion and force controller for manipulators with

uncertainties in both the robot and contact surfaces. Vukobratovic et al. (1996) consider the problem of simultaneous stabilization of both the robot motion and interaction force in Cartesian space after contact in robotic tasks. Tarn et al. (1996) use an event-driven switching control strategy for robot impact control and force regulation where the instant of impact must be known. They state that control of manipulator impact and contact is an important current research area. They present an excellent literature review of the subject: all of the reviewed methods require an artificial control mode change in the transition from free motion to contact.

Recently there has been a lot of work concerning haptic feedback in remote and/or virtual environments, including haptic interface development (Ishii et al., 1994), virtual object manipulation (Richard et al., 1996), multimodal feedback in design for assembly (Gupta et al., 1997), telerobotic architectures and applications (Ciscon et al., 1994 and Hunter et al, 1993), and substituting other sensory modes for force reflection (Massimino and Sheridan, 1993).

The current article presents a manipulator control method for effective task performance involving contact with the environment, the Naturally-Transitioning Rate-to-Force Controller (*NTRFC*). In free motion the manipulator moves with rate control, while in contact with the environment the force/moment wrench exerted on the environment is controlled, similar to Hogan's impedance controller with only the damping term. No artificial control mode or gain parameter changes are required so the transition is termed natural. A wrist-mounted F/T sensor and Force/Moment Accommodation (*FMA*) algorithm are required. Rate and *FMA* are active on all Cartesian axes simultaneously so no hybrid scheme is necessary. Since there are no artificial mode changes required, the threshold of contact is unimportant (the F/T sensor reading is fed back continuously).

The authors have implemented the *NTRFC* in an experimental system at Wright-Patterson AFB. The *NTRFC* method was implemented using the 3-degree-of-freedom (dof) PHANToM haptic interface

as the master, and a 6-dof Modular Expandable Robot Line (MERLIN) manipulator as the slave. The PHANToM could only command translational motion, but the *NTRFC* allowed for general spatial motion to relieve unwanted binding moments when the MERLIN contacted the environment, due to a 6-dof *FMA* algorithm. To the extent of the author's knowledge, this was the first time that the PHANToM was used for Cartesian force-reflecting teleoperation of a kinematically dissimilar remote manipulator. One known teleoperation was by SensAble Inc., using one PHANToM to drive another at the joint level.

The research problems addressed in this article are twofold: contacting the environment via rate control without artificial controller changes; and reducing the contact wrench (force/moment) in teleoperation tasks. This article presents the *NTRFC* approach to solve these research problems. The treatment is brief since the *NTRFC* algorithm has been presented in a conference paper (Williams and Murphy, 1998) and control algorithm and experimental system details are given in an Air Force report (Williams and Henry, 1998). This article concentrates on experimental evaluation and results of the *NTRFC* and force-reflecting teleoperation via multiple human teleoperator subjects. This data is new and has not been previously published; it is quite compelling in favor of the *NTRFC* with force-reflection to solve the stated research problems.

NATURALLY-TRANSITIONING RATE-TO-FORCE CONTROLLER (*NTRFC*)

The Naturally-Transitioning Rate-to-Force Controller (*NTRFC*) is a combination of resolved-rate control (Whitney, 1969) and force/moment accommodation (*FMA*) control enabled on all Cartesian axes at all times. The *NTRFC* can be applied to control any manipulator(s) with wrist-mounted force/torque sensor, rate inputs, and contact with the environment. The system behaves as a rate controller in free motion and as a force controller in contact. The transition requires no mode changes, logical switches, or gain changes in the controller software or hardware and thus is termed a natural transition. The *NTRFC* control diagram is given in Fig. 1.

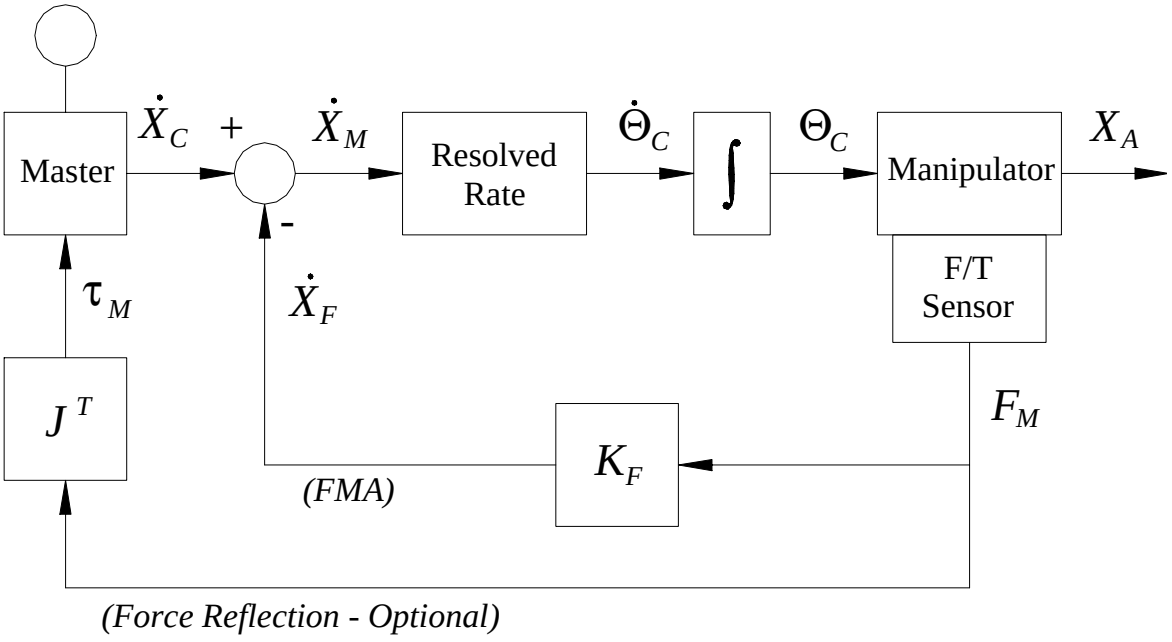

Figure 1. NTRFC *Control Diagram*

The displacement of the master device via the operator's hand is interpreted as a commanded Cartesian rate $\dot{X}_C$ to drive the slave manipulator motion. The total rate command $\dot{X}_M$ is sent to the resolved-rate algorithm which automatically calculates the required joint rates $\dot{\Theta}_C$ to achieve the required Cartesian motion $\dot{X}_M$. The resolved-rate algorithm is subject to singularities; this problem has

been handled by using a Singular-Value Decomposition (*SVD*) approach in place of the standard matrix Gaussian elimination when the determinant of the slave Jacobian matrix approaches zero. At each control cycle the commanded joint rates are integrated to commanded joint angles Θ_C which are sent to the slave manipulator joint servo controllers. One measure of the actual slave motion is the resulting Cartesian pose X_A (position and orientation; shown for conceptual purposes and not required in control). The six-axis F/T sensor mounted after the last slave joint continuously monitors the wrench reading F_M (after adjustments for static and inertial loading, and noise), regardless of whether the motion is free, constrained, or in transition between the two. The current wrench reading (after adjustments for static and inertial loading plus coordinate and rigid-body wrench transformations) is sent back the summing junction in Fig. 1 as $\dot{X}_F$, after it is multiplied by the *NTRFC* matrix gain K_F. This is the *FMA* loop which automatically drives the slave to feel zero contact wrench. The human operator can command a conflicting $\dot{X}_C$ (i.e. a direction to increase the contact wrench) and a stable equilibrium condition results where the slave exerts a constant wrench while the human hand is holding a steady $\dot{X}_C$. The description is now complete for the *NTRFC* algorithm. If the master device enables force-reflection, the optional outer loop in Fig. 1 is required to allow the operator to feel the (transformed and scaled) contact wrench F_M via the master Jacobian matrix transpose mapping.

In free motion, the displacement of the operator's hand on the master device is proportional to the Cartesian rate of the manipulator end-effector. In contact, the displacement of the operator's hand on the master device is proportional to the wrench exerted by the manipulator end-effector on the environment. No change in control mode is necessary since resolved-rate control and the *FMA* algorithm act simultaneously on all Cartesian axes, with a single set of gains. If force/moment reflection is enabled then the wrench of the operator's hand on the master device (reacting to the wrench reflection) is proportional to the wrench exerted by the manipulator end-effector on the environment.

EXPERIMENTAL SYSTEM

The *NTRFC* algorithm was implemented in hardware with a force-reflecting master to evaluate its effectiveness for remote teleoperation tasks. The experimental system implemented by the authors in the Human Sensory Feedback (HSF) Laboratory of Wright-Patterson AFB is discussed in this section.

A 3-dof PHANToM haptic interface, commercially available from SensAble Inc., is used as the master device (Fig. 2). The PHANToM has three motors that combine to exert *X*, *Y*, and *Z* forces on the user's fingertip; no moments are currently possible. Each motor has an optical encoder for angle sensing; from this information and forward kinematics, the *X*, *Y*, and *Z* translational position from a reference frame can be calculated and interpreted as $\dot{X}_C$ for Fig. 1. A passive 3-dof gimbal is attached to a thimble which interfaces to the user's fingertip. In the HSF lab, there are no encoders to read the gimbal orientation, which means the user may only input translation motion to the slave.

Figure 2. PHANToM Haptic Interface

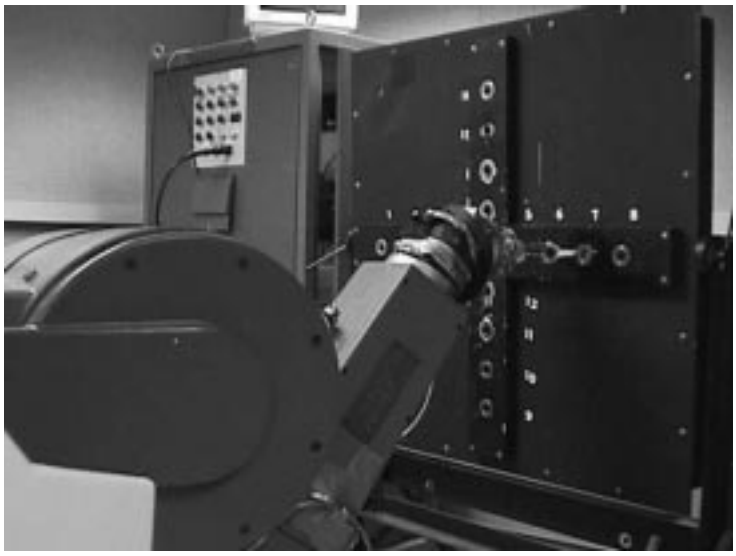

Figure 3. MERLIN Robot with Taskboard

A MERLIN industrial robot is the slave manipulator (Fig. 3). The left-handed MERLIN 6500 industrial robot arm (American Robot Corporation, 1985) in the HSF lab is a 6-dof spatial device

consisting of six revolute joints in series, driven by stepper motors. The MERLIN also has encoders on each motor which continuously measure joints angles, used in forward kinematics for rate and wrench coordinate and rigid-body transformations.

A standard Fitt's law (Fitts and Peterson, 1964) peg-in-hole taskboard provides the remote task (Figs. 3 and 4). Figure 4 shows that the operator is given two views of the MERLIN/Taskboard environment to accomplish the remote task via teleoperation. The basic task was to move the peg via teleoperation of the remote manipulator from a starting hole to an ending hole (all holes are equipped with detection switches at the same depth). The peg attached to the end of the MERLIN has the following coordinate conventions: X is normal to the taskboard (MERLIN approach direction) and Y and Z are in the plane of the taskboard (called the tangential directions in the results). The teleoperation control system is a distributed PC system. For details regarding the experimental system, see Williams and Henry (1998).

Figure 4. Taskboard in Operator Views

The experimental system is not general for spatial tasks since a 3-dof master commands a 6-dof slave. The peg-in-hole task requires only spatial translational motion (X, Y, and Z translational rates are commanded by the operator via the PHANToM), assuming good initial alignment of the MERLIN peg

with the taskboard. However, when the Naturally-Transitioning Rate-to-Force Controller (*NTRFC*) is used, the autonomous full 6-dof Force/Moment Accommodation (*FMA*) algorithm is enabled. This means that, though the user cannot command slave Cartesian angular motion via the PHANToM, the *FMA* algorithm can automatically perform slave Cartesian angular motions to relieve unwanted binding moments in contact. This scenario is termed Reduced-dof Teleoperation and has application to any tasks requiring primarily translational freedoms where binding moments are undesirable.

NTRFC AND FORCE REFLECTION EFFECTIVENESS EXPERIMENT

Objective

The purpose of this experiment was to test the effectiveness of four different control modes during PHANToM/MERLIN master/slave teleoperation, using a standard Fitts' law peg-in-hole task. The four control modes were pure rate control, rate control with force reflection, the Naturally-Transitioning Rate-to-Force Controller (*NTRFC*), and *NTRFC* with force reflection. The performance criteria were the task completion time and sum of the forces and moments exerted on the environment during the task. Our experimental hypothesis is stated below.

Experimental Hypothesis

For teleoperation tasks involving free motion and contact of the manipulator with the environment, where the desirable metrics are minimum task time and minimum exerted wrench during the task, the Naturally-Transitioning Rate-to-Force Controller (NTRFC) *with force reflection will perform the best, the* NTRFC *without force reflection will perform second-best, rate control with force reflection will perform third best, and pure rate control will perform the worst.*

Procedure

A standard peg-in-hole task was used to evaluate the effectiveness of the four control modes. Seven human subjects in the experiment used the PHANToM to control the MERLIN under one of the four control modes. The operator sat facing the remote viewing monitors with two different views of the taskboard, as seen in Fig. 4. The PHANToM was located just to the right of the monitor (also shown in Fig. 4), and the subject was facing away from the MERLIN.

The bottom of each hole in the taskboard contained a switch that was connected to a PC. The computer prompted the operator with a starting hole and a destination hole. When the switch in the starting hole was triggered the computer began timing, and when the destination hole switch was triggered the timer stopped. The task completion time and wrench history was then recorded in a file. The subjects were instructed to complete the task as fast as possible with minimum taskboard contact. Each subject was trained and allowed to practice with all four control modes prior to taking data. The effectiveness of the control modes was determined by the performance criteria: time for task completion, and the sum of the forces and moments exerted on the environment.

The experiment used seven subjects selected at random from a subject pool provided by the Air Force (non-expert subjects). Each subject performed six trials with each of the four control modes. Each trial consisted of six sections of four tasks, where a task was triggering the switch in the start hole and then the destination hole. Three of the sections used a peg with a 1.5 *cm* diameter, and the other three used a peg with 0.98 *cm* diameter. All holes have a 2 *cm* diameter. There were two different distances between start and destination holes, 48 *cm* and 8 *cm*.

Performance Measures

Task completion time. Task completion time was one of the performance measures used. Since it would not be meaningful to compare task completion times for different size pegs and different traversed distances, Fitts' law (Fitts and Peterson, 1964) was used to define the task difficulty. Equation (1) gives the index of difficulty formula.

$$I_d = LOG_2\left[\frac{2 * A}{D_h - D_p}\right] \tag{1}$$

where A is the distance traveled, D_h is the diameter of the hole, and D_p is the diameter of the peg. When the task completion time is plotted versus the index of difficulty a linear plot should result, unless the task is extremely difficult or easy. The index of difficulty has units of *bits*; therefore, the inverse slope of the line is the human/system baud rate. Baud rate defines the capacity to perform a task; for example, a human doing the peg-in-hole task directly has a baud rate of about 6 *bits*/*sec* (Fitts and Peterson,1964).

Sum of Forces. The second performance criterion was the sum of contact forces and moments in all Cartesian directions. Each control cycle (approximately every 0.006 *sec*), the wrench exerted on the environment was recorded. Later, the sum of the forces and moments in each direction was computed. It was important to keep the forces in different axes separate to see if the user reacted differently to normal or tangential forces. The forces and moments recorded from pure rate control were used as a baseline to determine a percent reduction (improvement) for the other modes. A large percent reduction in contact forces and moments is desirable. Equation (2) shows the definition for percent reduction.

$$\%R_i = \left(1 - \frac{\sum F_i}{\sum F_{rate_i}}\right) * 100\% \qquad i = X, Y, Z \qquad (2)$$

$\sum F_i$ is the summation of forces in a single Cartesian direction ($i = X, Y, Z$ separately) over task time for a given teleoperation control mode; $\sum F_{rate_i}$ is the same for the pure rate control mode baseline. This equation was used for each direction (X, Y, Z) of force and each direction (X, Y, Z) of moment. A weighted percent reduction was used to quantify the total percent reduction of forces (and, separately, moments). The weighted percent reduction was found using Eq. (3).

$$W\%R = \sum_{i=X,Y,Z} \left(\%R_i * \frac{\sum F_i}{\sum_{j=X,Y,Z} F_j} \right) \quad (3)$$

This measure yields a more conservative value than the single-direction percent reductions of Eq. (2).

Results

Figure 5 shows the average task completion times vs. task difficulty for the four teleoperation control modes. The graph shows the order from fastest to slowest average task times was generally rate control with force reflection, pure rate control, *NTRFC* with force reflection, and finally *NTRFC*. However, the maximum difference was only 0.3 *sec*, which is negligible considering total task times of 8 to 20 *sec*. When fitting the data with the best straight line, the slopes of all the lines were almost identical, resulting in a baud rate of 0.282 bits/*sec*, much lower than the human alone (approximately 6 bits/*sec*). On the graphs in this section, the following notation is used to distinguish control modes: **Rate** (pure rate control), **Rate/FR** (rate control with force reflection), **NTRFC** (*NTRFC*), and **NTRFC/FR** (*NTRFC* with force reflection).

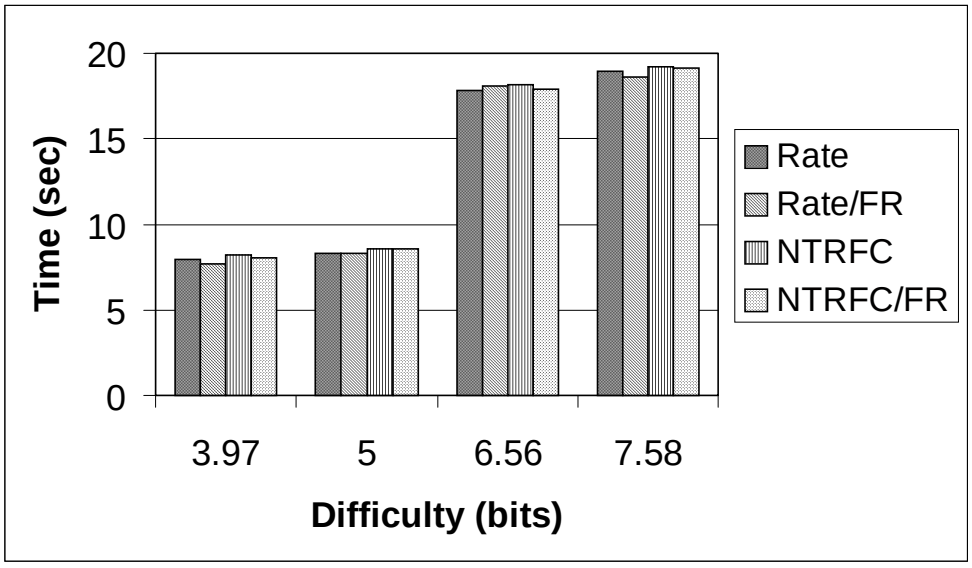

Figure 5. Average Task Completion Times vs. Index of Difficulty

Figures 6 and 7 show the percent reduction of forces and moments, taken in single directions, as defined by Eq. (2). Pure rate control always yielded the highest forces and moments (thus justifying its use as the baseline) and rate control with force reflection followed close behind. The *NTRFC* shows a large reduction of forces and moments, but the combination of *NTRFC* with force reflection had the largest reduction (lowest forces and moments) of all four modes. The percent reduction in the normal direction (*X*) was 0.6%, 28.5%, and 35.3% for force reflection, *NTRFC*, and *NTRFC* with force reflection, respectively. However, this was much lower than the reductions in the tangential directions (*Y* and *Z*). The *Y* percent reductions were 24.3%, 70.3%, and 74.9% and the *Z* percent reductions were 20.9%, 66.1%, and 70.5% for force reflection, *NTRFC*, and *NTRFC* with force reflection. The tangential direction percent reductions were approximately double that of the normal direction percent reductions for *NTRFC* and *NTRFC* with force reflection. The disparity was even greater for the force reflection mode, where there was little reduction in the normal direction and over 20% reduction in the tangential directions. This can be explained by the nature of the human body. Humans are much stronger pushing away from their bodies (normal direction) than they are pushing right, left, up, or down (tangential directions). This means a small force in the tangential directions would push the operators finger in that direction thus helping relieve the force exerted by the slave on the environment, and it would take a much larger force to achieve the same result in the normal direction.

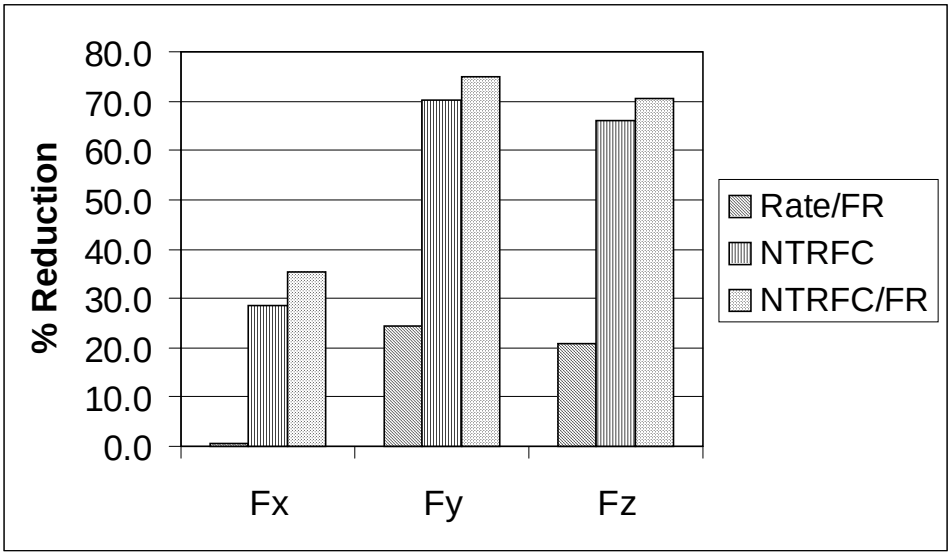

Figure 6. Percent Reduction for Forces X Y Z

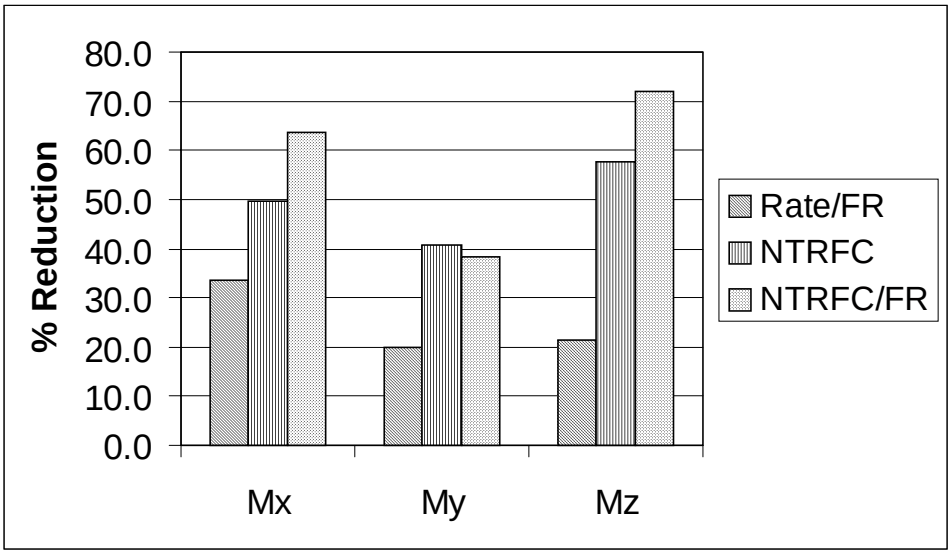

Figure 7. Percent Reduction for Moments X Y Z

Figure 8 shows the weighted percent reduction for the same forces and moments data (using Eq. (3)). The purpose of this graph is to quantify the overall effectiveness of each mode in reducing the binding wrench, using a more conservative, combined-direction measure. Force reflection was able to reduce the combined forces by 6.6% and the combined moments by 25.3%, *NTRFC* reduced the combined forces by 35.3% and the combined moments by 49.8%, and *NTRFC* with force reflection was able to reduce the combined forces by 41.5% and the combined moments by 52.0%. The control

methods were able to reduce the combined moments by 18.9%, 14.5%, and 10.6% more than they were able to reduce the combined forces for force reflection, *NTRFC,* and *NTRFC* with force reflection, respectively.

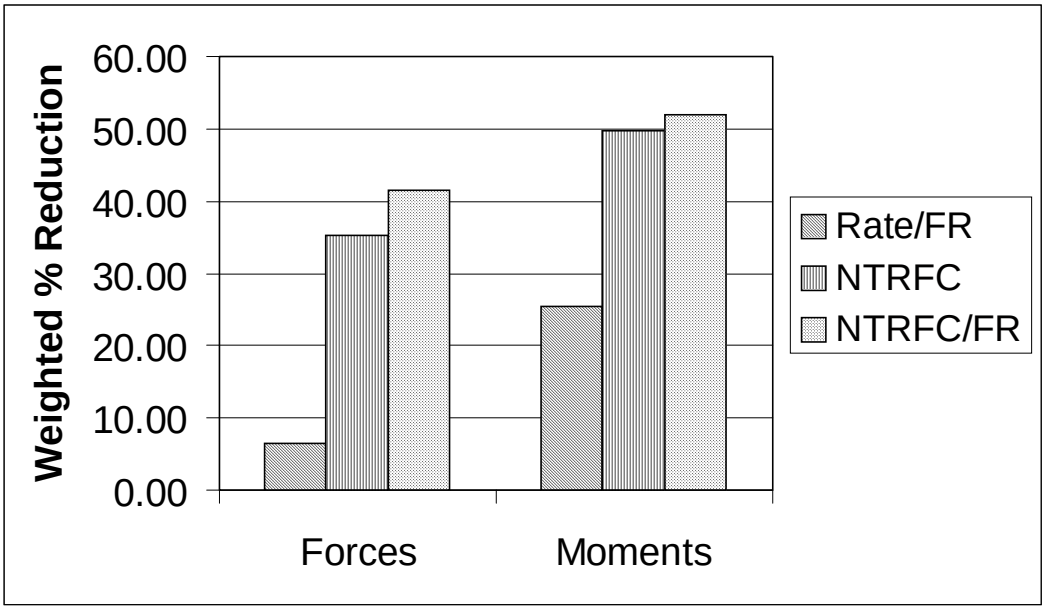

Figure 8. Weighted Percent Reduction for Combined Forces and Combined Moments

The reduction in the sum of the forces and moments could be caused by a reduction in the magnitude of the forces and moments, a reduction in the duration of contact with the environment, or a combination of both. Figure 9 shows the percent reduction for average maximum forces and moments (by single directions). The moment about the *X*-axis was not included because these values were very small (about the peg, there is very little contact and friction). Note the Rate/FR mode in the F_Y direction yielded a small negative percent reduction; this is the only instance in which a mode is (slightly) worse than the baseline Rate mode. Pure rate control and rate control with force reflection were very similar in maximum forces and moments, but the *NTRFC* and *NTRFC* with force reflection showed significant

reduction in both maximum forces and moments. Again, note that the percent reductions in the tangential force directions (*Y* and *Z*) were double that of the normal force direction (*X*) all modes.

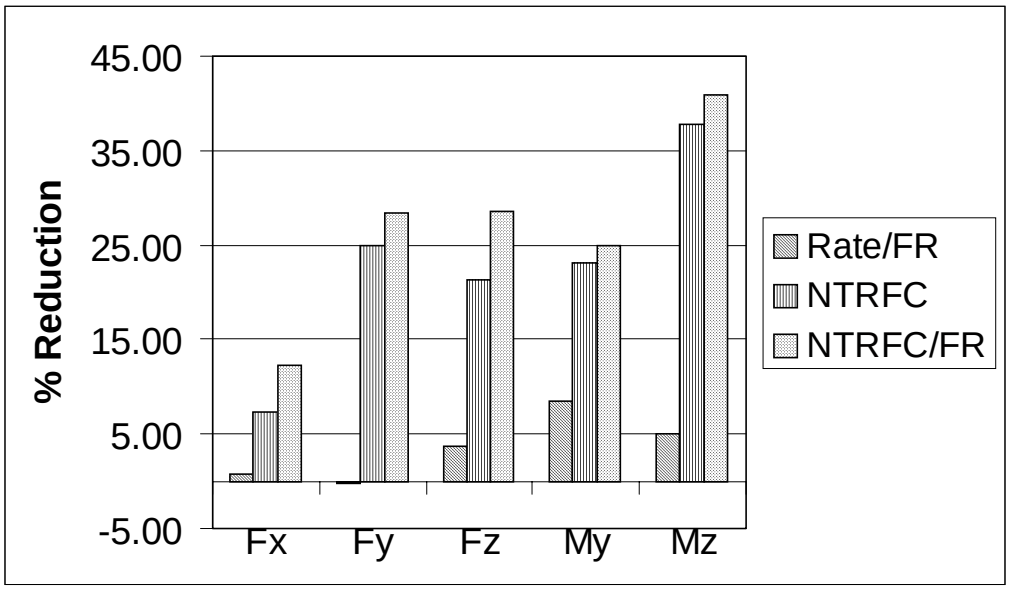

Figure 9. Percent Reduction of Average Maximum Forces and Moments (by Single Directions)

Figure 10 shows the reduction in duration of contact for both the forces and moments (by single directions). Again the *NTRFC* and *NTRFC* with force reflection perform much better than rate control with force reflection (which is only a small reduction from the pure rate control baseline). It should again be noted that the tangential force directions (*Y* and *Z*) show double the reduction of the normal force direction (*X*). When the reductions of the maximum forces and moments are compared with the reductions in duration of contact it can be seen that the reduction in contact duration is approximately double that of the maximum forces and moments.

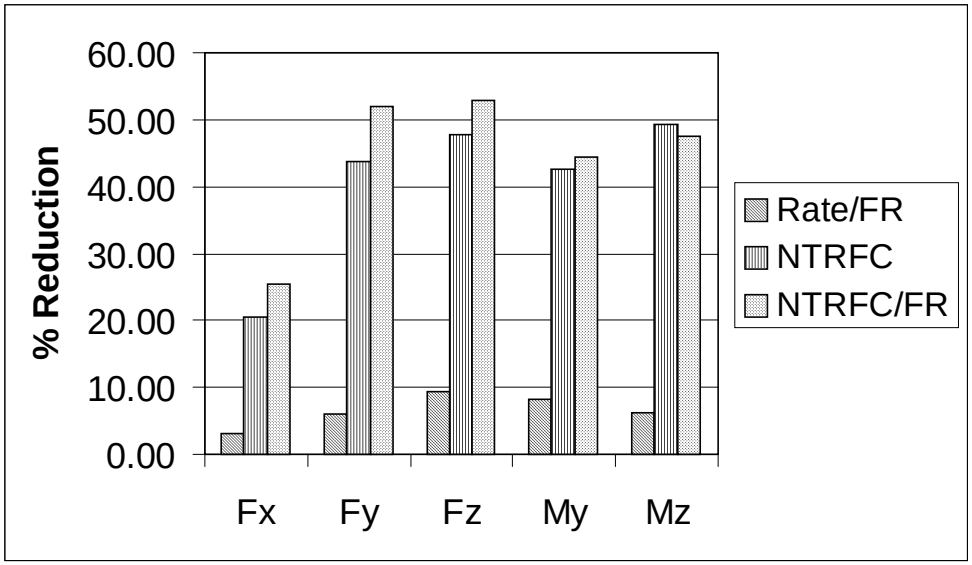

Figure 10. Percent Reduction in Average Contact Duration for Forces and Moments (by Single Directions)

Again, the total percent reduction of maximum forces and moments and contact duration for forces and moments was quantified with the more conservative weighted percent reduction formula. Figure 11 shows the weighted percent reduction of combined maximum forces and moments, and Fig. 12 shows the weighted percent reduction for contact duration. Force reflection was able to reduce the maximum force by 1.2% and maximum moment by 6.6%, the *NTRFC* was able to reduce the maximum force by 10.50% and maximum moment by 29.6%, and the *NTRFC* with force reflection performed the best by reducing the maximum force by 15.4% and maximum moment by 31.9%. It should be noted that the reduction of forces was less than half of the reduction of moments in all cases. The duration of contact was reduced even more than the maximum forces and moments. The reduction for force reflection was 5.5% and 16.5% for force duration and moment duration, the reduction for *NTRFC* was 33.0% and 52.1% for force duration and moment duration, and *NTRFC* with force reflection reduced the force duration by 38.3% and the moment duration by 51.8%.

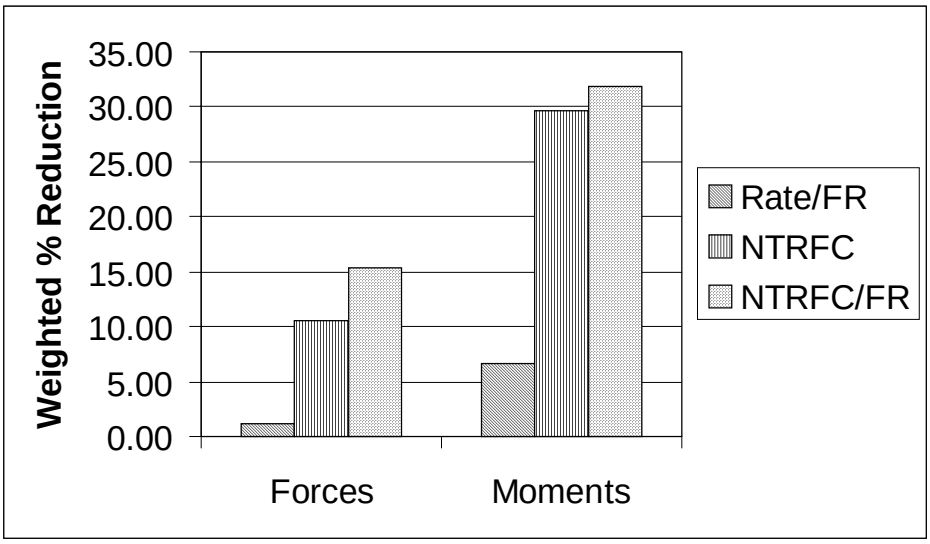

Figure 11. Weighted Percent Reduction of Combined Maximum Forces and Moments

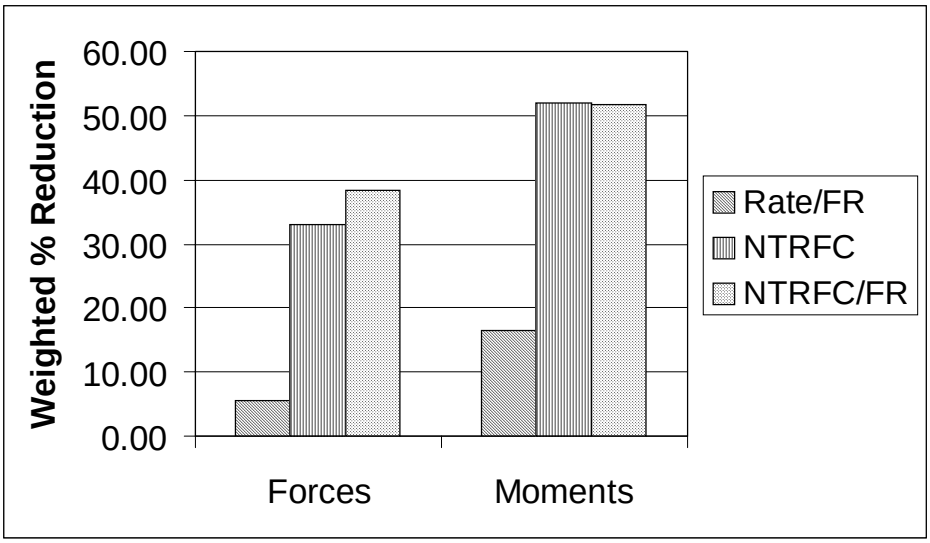

Figure 12. Weighted Percent Reduction of Contact Duration for Forces and Moments

Thus far all force and moment data for the four control modes has been presented in terms of percent reduction from the baseline (pure rate control). Table 1 presents the maximum contact forces and moments in physical units for the four control modes (averaged over all subjects and tasks). The moment about the *X*-axis (the peg axis) was not included because the moments were very small. With the exception of the force F_X in the insertion direction, the other forces and moments are relatively small. This could call into question the significance of our results. However, since the results were

averaged over all subjects and tasks we believe the results are significant. Also, the environment was compliant (the entire board would shift as a rigid body if the force was too high) and the peg had a built-in physical spring. This was done to protect the robot system from damage since this was the first series of experiments in this area. We believe that our results would be even more favorable for *NTRFC* with force reflection in a very rigid environment with higher contact forces and moments.

Table 1. Average Maximum Forces (lb) and Moments (in-lb)

	Rate	Rate with Force Reflection	*NTRFC*	*NTRFC* with Force Reflection
F_X	27.41	27.19	25.39	24.07
F_Y	4.34	4.35	3.26	3.11
F_Z	3.81	3.67	3.00	2.72
M_Y	4.17	3.82	3.21	3.13
M_Z	4.11	3.91	2.56	2.43

Now we present a discussion regarding the variability of the experimental data. The standard deviation is often used as a measure of the variability, but this can be misleading when comparing variables with different magnitudes, which is the case here for both task completion time and sum of forces and moments. The coefficient of variation (*COV*) is a normalized measure of the dispersion of data, and is calculated using Eq. (4).

$$COV = \frac{\sigma_{n-1}}{\mu} \tag{4}$$

Where $\sigma_{n\text{-}1}$ is the standard deviation for a data set and μ is the mean. This formula takes into account the fact that as the mean increases the standard deviation should increase proportionally. *COV* is dimensionless. When taking data for human factors experiments a coefficient of variation of 0.4 or less is considered acceptable in the Human Sensory Feedback Laboratory.

The coefficients of variation for the task completion times (whose averages were given in Fig. 5) are given in Table 2, for the four teleoperation control modes in the experiment. The *COV* ranged from 0.201 for rate control mode at 6.56 bits of difficulty to 0.285 for *NTRFC* with force reflection at 5 bits of difficulty. This is a small range with all *COV* below 0.4, indicating that the experimental time data is acceptable with respect to variability.

Table 2. Coefficients of Variation for Task Completion Times

Difficulty (bits)	Rate	*NTRFC*	Rate with Force Reflection	*NTRFC* with Force Reflection	Average
3.97	0.240	0.278	0.253	0.260	0.258
5.00	0.261	0.270	0.273	0.285	0.272
6.56	0.201	0.223	0.221	0.224	0.217
7.58	0.229	0.229	0.235	0.236	0.232
Average	0.233	0.250	0.245	0.251	0.245

Tables 3 and 4 show the coefficients of variation for the sum of forces and the sum of moments, respectively, for the four teleoperation modes. The *COV* for the forces ranged from 0.196 for rate control with force reflection in the *X* (normal) direction to 0.477 for rate control in the *Y* (tangential) direction. Three of the coefficients exceeded 0.4: 0.477 (Rate, F_Y); 0.436 (Rate, F_Z); and 0.451 (*NTRFC*, F_Y). However, the average *COV* for each control mode was below 0.4. The *COV* range for the moments was larger, from 0.18 for *NTRFC* with force reflection about *X* to 0.763 for *NTRFC* about *Z*. Two were above 0.4: 0.625 (*NTRFC*, M_X) and 0.763 (*NTRFC*, M_Z). For moments, the average *COV* for *NTRFC* is above 0.4; *COV* averages for the remaining three modes were below 0.4.

Table 3. Coefficients of Variation for Sum of Forces

Direction	Rate	*NTRFC*	Rate with Force Reflection	*NTRFC* with Force Reflection	Average
F_X	0.213	0.230	0.196	0.217	0.214
F_Y	0.477	0.451	0.357	0.258	0.386
F_Z	0.436	0.340	0.381	0.354	0.378
Average	0.375	0.340	0.311	0.276	0.326

Table 4. Coefficients of Variation for Sum of Moments

Direction	Rate	*NTRFC*	Rate with Force Reflection	*NTRFC* with Force Reflection	Average
M_X	0.358	0.625	0.323	0.180	0.372
M_Y	0.286	0.251	0.224	0.275	0.259
M_Z	0.383	0.763	0.359	0.276	0.446
Average	0.342	0.546	0.302	0.244	0.359

The higher coefficients of variation for the sum of forces and moments could be due to several factors. A primary reason for the sum of forces having higher *COV* is the accuracy with which the subject placed the peg in the hole. Some subjects were more accurate (not hitting the sides of the hole upon entrance). This can be seen by looking at the *COV* for directions alone. The average for the normal direction (*X*) was 0.214, but for the tangential directions it was 0.386 and 0.378 for the *Y* and *Z* directions, respectively. This accuracy likewise affects the moments. The average for the moments was 0.372, 0.259, and 0.446 about the *X*, *Y*, and *Z* axes, respectively.

Discussion

The variability analysis revealed that most of the experimental data was reasonable, defined as having a *COV* of less than 0.4. The experimental results showed that there was negligible difference in task completion time between the four different control modes. When looking at the force and moment data pure rate control performed the worst. The force reflection was able to reduce the sum of the contact forces by 6.6% and the sum of the moments by 25.3%. (All results in this discussion section are the more conservative combined-direction weighted percent reduction measures presented above.) The *NTRFC* was second-best reducing the sum of the forces by 35.3% and the moments by 49.9%. The *NTRFC* with force reflection performed the best by reducing the sum of the forces by 41.5% and the moments by 52.0%. The forces and moments in all cases were reduced more in the tangential directions than in the normal direction. The contact forces and moments were relatively small (with the exception of the force in the insertion direction) by design of the experiment (with significant environmental compliance) to protect the experimental hardware. We believe that our results would be even more pronounced in favor of *NTRFC* with force reflection when using a more rigid environment.

It was found that the reduction in forces and moments was the result of both a reduction in the average maximum forces and moments and a reduction of the duration of contact with the environment. Force reflection reduced the maximum contact forces by 1.2% and the maximum moments by 6.6%. The *NTRFC* reduced the maximum contact forces by 10.5% and the maximum moments by 29.6%. Finally, the *NTRFC* with force reflection reduced the maximum contact forces by 15.4% and the maximum moments by 32.0%. The contact durations were reduced even more than the maximum forces and moments. Force reflection reduced the duration of contact by 5.5% for the forces and 16.5% for the moments. The *NTRFC* reduced the contact duration for forces by 33.0% and the duration for moments

by 52.1%. The *NTRFC* with force reflection reduced the duration of contact forces by 38.3% and the duration of moments by 51.8%.

The task times did not show a significant difference for the four control modes. This is because the task was rather short and simple. For more involved tasks requiring 6-dof input and multiple contact steps, the *NTRFC* will likely yield faster task times, based on our experience in the lab.

The percent reduction of contact forces and moments did show a significant difference for the four control modes. The reasons for this are self-evident. The purpose of the force-moment accommodation (*FMA*) algorithm is to minimize the contact forces and moments during teleoperation. *FMA* is the key ingredient behind the *NTRFC*. If we use force reflection in addition to the *NTRFC*, not only will the *FMA* automatically try to minimize contact forces and moments, but the human operator will also feel the magnitudes of forces and moments exerted. Thus, the human can modify input commands with respect to minimizing the contact wrench.

The original hypothesis was proven based on the experimental performance criteria. The order of teleoperation control modes from best to worst is as follows:

- *NTRFC* with Force Reflection **(BEST)**
- *NTRFC*
- Rate Control with Force Reflection
- Pure Rate Control **(WORST)**

CONCLUSION

The research problems addressed in this article are: 1) contacting the environment via rate control without artificial controller changes; and 2) reducing the contact wrench in remote tasks via teleoperation. This article presents the Naturally-Transitioning Rate-to-Force Controller (*NTRFC*) approach to solve both of these research problems. With the *NTRFC*, the displacement of the operator's hand is proportional to the slave Cartesian rate in free motion. In contact, the displacement of the operator's hand is proportional to the slave wrench exerted on the environment. If force reflection is used, the wrench of the operator's hand is proportional to the slave wrench exerted on the environment.

The *NTRFC* was implemented in hardware at Wright-Patterson AFB. Experiments were conducted to determine the task time and wrench exertion performance of four teleoperation control modes: 1) rate control only (the baseline); 2) rate control with force reflection; 3) *NTRFC*; and 4) *NTRFC* with force reflection. The experimental hypothesis was validated by the results (averaged for seven human teleoperator subjects with multiple trials for each control mode and peg-in-hole task): *NTRFC* with force reflection performed the best and rate control only performed the worst with respect to exerting low wrenches on the environment during task performance. A second performance criterion was task time; time differences amongst the four control modes were negligible.

A weighted percent reduction measure in exerted forces and moments was presented to compare the four modes. It was discovered that moments were reduced more than forces and the forces in the plane of the taskboard were reduced more than the normal force. The reduction in the sum of the forces and moments is caused by a combination of both a reduction in the magnitude of the forces and moments and a reduction in the duration of contact with the environment. The experimental results show the *NTRFC* with force reflection is a powerful teleoperation control mode for minimum wrench exertion in teleoperation tasks with free motion and contact.

ACKNOWLEDGEMENTS

This research was supported by a grant from the Human Sensory Feedback Laboratory at Wright-Patterson AFB and the AFOSR Summer Faculty Research Program. The authors thank Jim Berlin for implementation assistance.

REFERENCES

American Robot Corporation, 1985, "*Service manual for the System II Merlin Intelligent Robot*".

L.A. Ciscon, J.D. Wise, and D.H. Johnson, 1994, "*A Distributed Data Sharing Environment for Telerobotics*", Presence 3(4): 321-340.

R. Colbaugh, H. Seraji, and K. Glass, 1993, "*Direct Adaptive Impedance Control of Robot Manipulators*", Journal of Robotic Systems, 10(2): 217-248.

P.M. Fitts and J.R. Peterson, 1964, "*Information Capacity of Discrete Motor Responses*", Journal of Experimental Psychology, 67 (2), 103-112.

R. Gupta, T.B. Sheridan, and D. Whitney, 1997, "*Experiments Using Multimodal Virtual Environments in Design for Assembly Analysis*", Presence 6(3): 318-338.

N. Hogan, 1985, "*Impedance Control: An Approach to Manipulation (3 parts)*", ASME Journal of Dynamic Systems, Measurement, and Control, 107:1-24.

I.W. Hunter, T.D. Doukoglou, S.R. Lafontaine, P.G. Charette, L.A. Jones, M.A. Sager, G.D. Mallinson, and P.J. Hunter, 1993, "*A Teleoperated Microsurgical Robot and Associated Virtual Environment for Eye Surgery*", Presence 2(4): 265-280.

J.M. Hyde and M.R. Cutkosky, 1994, "*Controlling Contact Transition*", IEEE Control Systems Magazine, 14(1): 25-30.

M. Ishii, M. Nakata, and M. Sato, 1994, "*Networked SPIDAR: A Networked Virtual Environment with Visual, Auditory, and Haptic Interactions*", Presence 3(4): 351-359.

M.J. Massimino and T.B. Sheridan, 1993, "*Sensory Substitution for Force Feedback in Teleoperation*", Presence 2(4): 344-352.

M. Raibert and J.J. Craig, 1981, "*Hybrid Position/Force Control of Manipulators*", ASME Journal of Dynamic Systems, Measurement, and Control.

P. Richard, G. Birebent, P. Coiffet, G. Burdea, D. Gomez, and N. Langrana, 1996, *"Effect of Frame Rate and Force Feedback on Virtual Object Manipulation"*, Presence 5(1): 95-108.

T.J. Tarn, Y. Wu, N. Xi, and A. Isidori, 1996, "*Force Regulation and Contact Transition Control*", IEEE Control Systems Magazine, 16(1): 32-40.

M. Vukobratovic and R. Stojic, 1996, "*On Position/Force Control of Robot Interacting with Dynamic Environment in Cartesian Space*", ASME Journal of Dynamic Systems, Measurement and Control, 118(1): 187-92.

D.E. Whitney, 1969, *"Resolved Motion Rate Control of Manipulators and Human Prostheses"*, IEEE Transactions on Man-Machine Systems.

R.L. Williams II and M.A. Murphy, 1998, *"Naturally-Transitioning Rate-to-Force Control"*, CD Proceedings of the 1998 ASME Design Technical Conferences, 25th Biennial Mechanisms Conference, Atlanta, GA, September 13-16.

R.L. Williams II and J.M. Henry, 1998, *"PHANToM / Merlin Force-Reflecting Teleoperation: Theory and Implementation"*, Final Report, AFOSR Summer Research Program.

B. Yao and M. Tomizuka, 1995, "*Adaptive Control of Robot Manipulators in Constrained Motion - Controller Design*", ASME Journal of Dynamic Systems, Measurement and Control, 117(3): 320-328.